CERN Summer Student Programme
Project Report

15. August 2025

Characterisation of Silicon Carbide (SiC) Pixel Detectors

Basil Wymann

Supervisors:
Roman Müller
Susanne Kühn

Contents

1 Introduction

This report presents the characterization of silicon carbide (SiC) pixel detector samples, carried out as part of the CERN Summer Student Programme 2025. The focus lies on the measurement of noise levels and the detection of α- and β-radiation. While the overall project also included tasks such as the calibration of amplifiers and the development of Python scripts for automated measurements, these aspects are not discussed in detail here.

Silicon pixel detectors are a well-established technology used in high-energy physics experiments, such as the inner tracker of the ATLAS detector. Their small pixel size provides high spatial resolution, on the order of 10 µm [1]. However, because of the close proximity of the pixels to the collision points of the protons, there is a strong radiation exposure. As a result, the silicon pixel detectors in ATLAS break down over time. Thus, new materials with better radiation hardness are explored: Silicon carbide (SiC) is one candidate to potentially offer higher robustness against radiation [2]. Additionally, SiC offers the advantage of having a higher bandgap than silicon, such that the leakage current of the detectors could be reduced. As a result, noise and heat generation can be reduced. Due to these benefits combined with new advances in the fabrication of SiC devices, SiC pixel detectors are a promising technology to replace or complement Si pixel detectors in future detectors [3].

1.1 Silicon Carbide Pixel Detectors

Silicon carbide (SiC) pixel detectors function fundamentally as semiconductor diodes. A conceptual cross-sectional schematic is shown in Figure 1. However, the precise internal structure of the specific samples studied in this project is not disclosed.

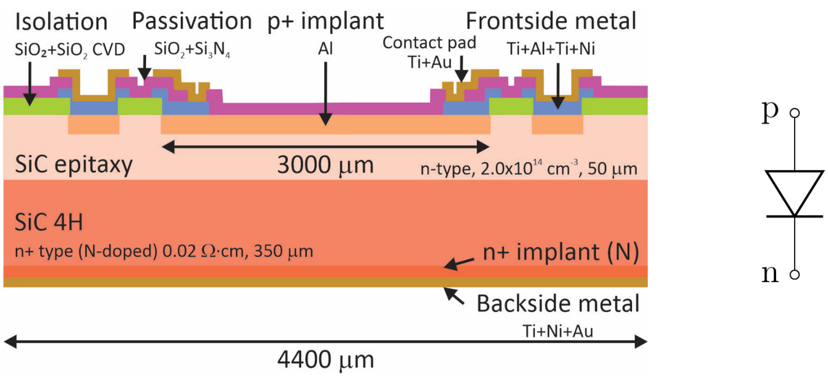

Figure 1: A cross-sectional schematic of the investigated SiC detectors could look something like this. Reproduced from [2].

When a high-energy particle traverses the diode, it deposits energy that generates electron-hole (e-h) pairs within the depleted region. Under reverse bias operation - commonly used in such detectors - an electric field is established across the junction.

This field drives the electrons toward the n-doped electrode and the holes toward the p-doped electrode, resulting in a transient current. The detection of this current pulse signifies the passage of a high-energy particle [3].

The energy required to create an e-h pair in SiC ranges from 7.6 to 8.4 eV [3], significantly higher than the 3.6 eV required in silicon [3]. Consequently, for a given deposited energy, SiC detectors produce fewer charge carriers than silicon detectors. This results in a weaker output signal for SiC-based detectors compared to their silicon counterparts [3].

1.2 Experimental setup

A simplified version of the experimental setup is illustrated in Figure 2. Two SiC pixel detectors were characterized: IHEP_Sample3_6-2, which will be referred to as "IHEP", and CNM_SiC_16886_W4_EPI_100_PAD_-4_8, referred to as "CNM". Different radiation sources were used to irradiate the SiC samples: ^{241}Am with 38.93 kBq or 57.58 Bq for α- and ^{90}Sr with 21.56 MBq for β-radiation.

The high-energy particles from these sources generate signals inside the SiC detectors that were amplified directly on the UCSC board [4], onto which the SiC samples were bonded. The amplified signal was recorded with a *Tektronix 6 Series MSO* oscilloscope with a bandwidth of 2.5 GHz. A *Keithley 2470* high-voltage source was used to apply the bias voltage to the SiC diode. A *Aim TTi PL601-P* power supply provided the 2.25 V supply voltage for the UCSC amplifier.

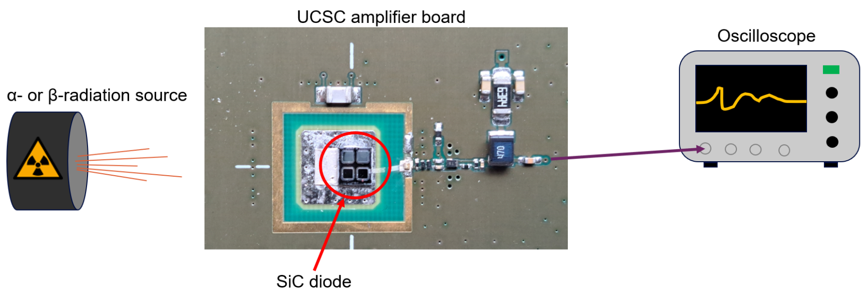

Figure 2: Experimental setup for the characterisation of the SiC detectors.

In an initial experiment, not described further in this report, the UCSC amplifiers were calibrated: The output charge of the amplifier (obtained by integrating the output current over time) was found to be approximately 8 times higher than the charge injected into the input port of the amplifier (which should approximately be equal to the charge generated inside the SiC detector).

2 Measurement of Noise Level

The objective of this experiment is to characterize the noise level of the output signal from the UCSC amplifier. Understanding baseline noise is essential for determining the minimum signal strength of a detection event that can be reliably distinguished from noise. For this measurement, no radiation source was applied.

The noise level was recorded for an UCSC board without a SiC sample bonded on it, as well as two boards with the two samples CNM and IHEP. Different bias voltages were applied on these SiC samples. The measured root mean square (RMS) values of the output signal for the different configurations are indicated in Table 1.

Sample	Bias voltage (V)	RMS (mV)
None	-	0.172
CNM	0	0.195
	80	0.189
IHEP	0	0.209
	80	0.206

Table 1: RMS values of the noise level for different configurations.

The results indicate that bonding SiC samples to the UCSC board increases the noise level. This is likely due to coupling from bonding wires, which may act as antennas and pick up environmental noise, or from noise introduced via the high-voltage bias connection. Different bias voltages do not seem to have a significant effect on the noise level.

In addition, acquisition rates were measured for different trigger levels of the oscilloscope. The results of some measurements are shown in Figures 3(a) and 3(b). The general trend that the acquisition rate is very low for trigger levels above 1 mV is present for all configurations.

Note that smartphones or laptops connected to WiFi can significantly increase the noise level. It has been observed that it can lead to trigger rates of ∼60 Hz at a trigger level of 1 mV.

(a)

(b)

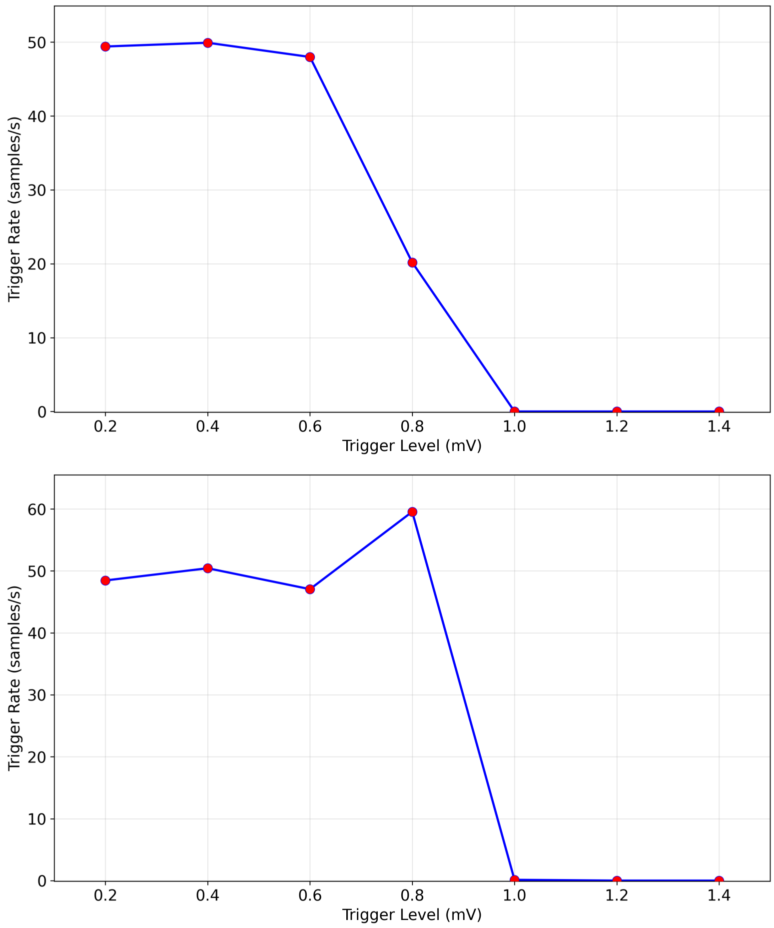

Figure 3: Acquisition rates for different trigger levels for two different configurations: (a) Only the UCSC board without any SiC sample and (b) the UCSC board with the CNM sample and 80 V bias voltage.

3 Detection of α-Particles

This chapter presents results from measurements of the detection of α-particles. Since α-particles from the ^{241}Am-source have a high energy of 5.486 or 5.443 MeV [5], we expect the generation of approximately 680'000 e-h pairs (= energy of the particle divided by the energy required to create one e-h pair; assuming that all of the kinetic energy of the α-particle is converted into the excitation of electrons).

3.1 Results for the CNM sample

The α-particles generate strong signals that are clearly above the noise level (Figure 4). Higher bias voltage results in a stronger average signal. This is likely due to a more efficient charge extraction for a higher bias voltage. The faster fall time at higher bias voltage may be attributed to the lower junction capacitance (due to the wider depletion region).

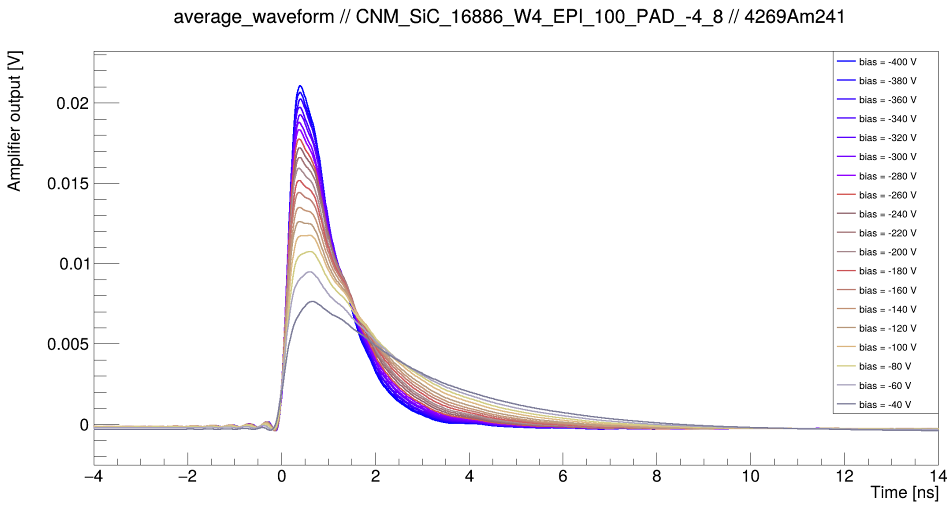

Figure 4: Average of 25'000 recorded waveforms from α-particle detection for different bias voltages.

The histograms in Figures 5(a) and 5(b) confirm that the peak height and output charge increase with stronger bias voltage. Note that a charge of 80 fC corresponds to $\sim$ 500'000 elementary charges, which is on the order of the expected 680'000 elementary charges.

For this measurement, a source with a high rate of radioactive decays (38.93 kBq) was used, which allowed for a quick recording of a high number of waveforms that required approximately 10 minutes per voltage step.

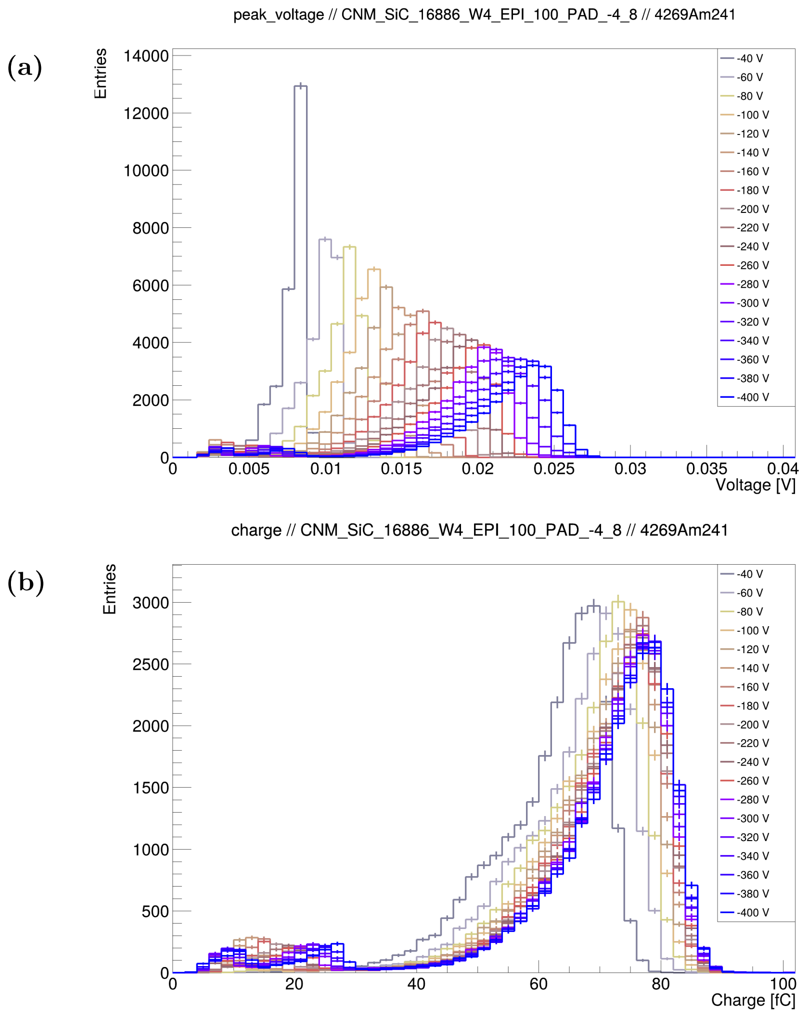

Figure 5: Histograms for the 25’000 recorded waveforms for each bias voltage: (a) measured peak-voltage of the pulse & (b) calculated extracted charge by integrating the output signal of the UCSC amplifier over time and dividing by the calibration factor (≈ 8).

3.2 Results for the IHEP sample

For the IHEP sample, it was not possible to perform the same measurements using the identical radiation source: For unknown reasons, the current flowing from the high-voltage source through the SiC detector fluctuated strongly and sometimes exceeded current compliance. By using another ^{241}Am-source with the lower rate of radioactive decays (57.58 Bq), this problem could be solved. However, due to the lower radioactivity, the recording of 25'000 particle detections took approximately 12 hours (25'000 waveforms were recorded for each step in the sweep of the bias voltage to obtain a high statistical significance). Therefore, the sweep of the bias voltage was restricted to only two values: 60 and 80 V.

The results are shown in Figures 6 and 7. They show the same trends as observed for the CNM sample.

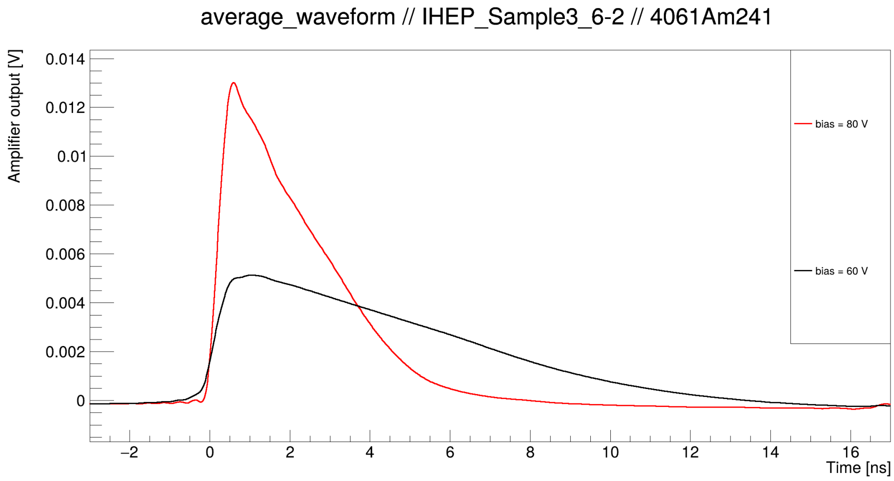

Figure 6: Average of 25'000 recorded waveforms from α-particle detection.

(a)

(b)

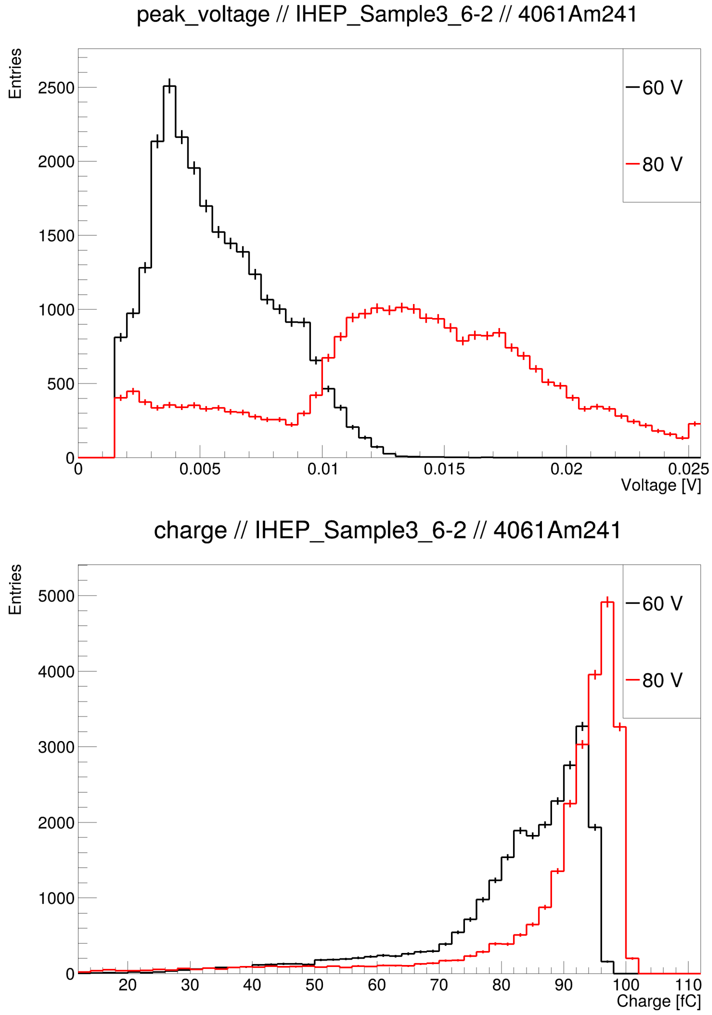

Figure 7: Histograms for (a) peak-voltage and (b) charge for the two bias voltages of 60 and 80 V.

4 Detection of β-Particles

The detection of β-radiation is more challenging because of the lower energy of the particles and the consequently smaller number of generated e-h pairs. The β-particles from the ^{90}Sr-source have an average energy of 0.3 MeV and a maximum energy of 2.2 MeV [6], which is much lower compared to the $\sim$5.45 MeV of the α-particles from the previous experiment. Therefore, it was not clear in advance whether the detection of β-radiation would even be possible. The trigger level of the oscilloscope was set to 1.2 mV. This should allow for the detection of relatively weak signals, while the number of triggering events due to noise can be neglected.

4.1 Results for the CNM sample

For β-radiation, the average waveforms (Figure 8) show less variation for different bias voltages compared to the previous experiment with α-radiation. One trivial reason for this is the smaller sweep range of the bias voltage: the minimum voltage is 160 V (as opposed to 40 V in the previous experiment). The reason for that is that the triggering rate was too low to get a sufficiently high number of waveforms (25'000) in reasonable time for weaker bias voltages.

As in the previous experiment, the fall time is reduced for stronger bias voltages (likely again due to the lower junction capacitance). However, the peak height is much lower than in the previous experiment (only $\sim$0.2 mV above the trigger level)and does not strongly increase with increasing bias voltage.

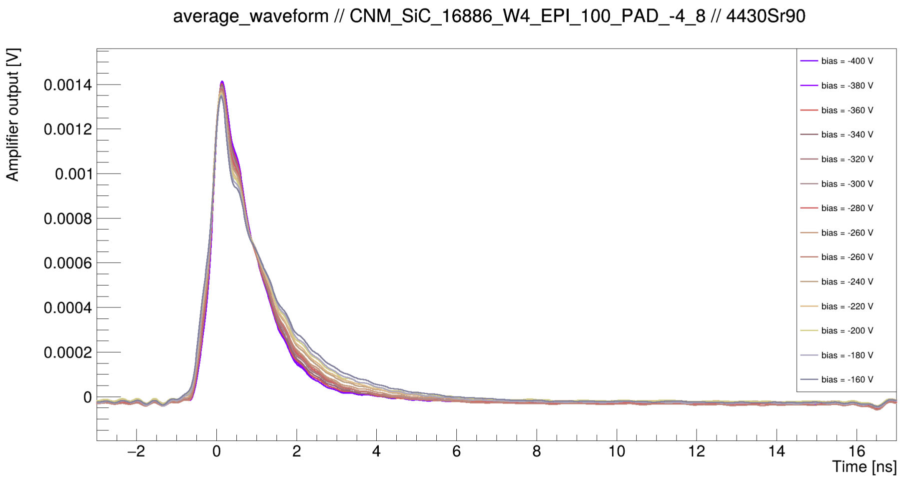

Figure 8: Average of 25'000 recorded waveforms from β-particle detection.

The lower peak height in general was expected and can be explained by the lower energy of the β-particles and the resulting smaller charge generated in the SiC detector (compare with Figure 9(b)).

A possible explanation for the surprisingly small change in the average peak height is that while particles with fixed energy produce higher peak voltages at increased bias, higher bias also allows the detection of lower-energy particles. These lower-energy particles generate signals just above the trigger level, which would not be recorded at lower bias. Thus, higher bias voltages help to detect more particles, even though the average peak voltage remains roughly the same. This also implies that there is a large share of β-particles that are not detected because the peak height of the resulting signal is below the trigger threshold.

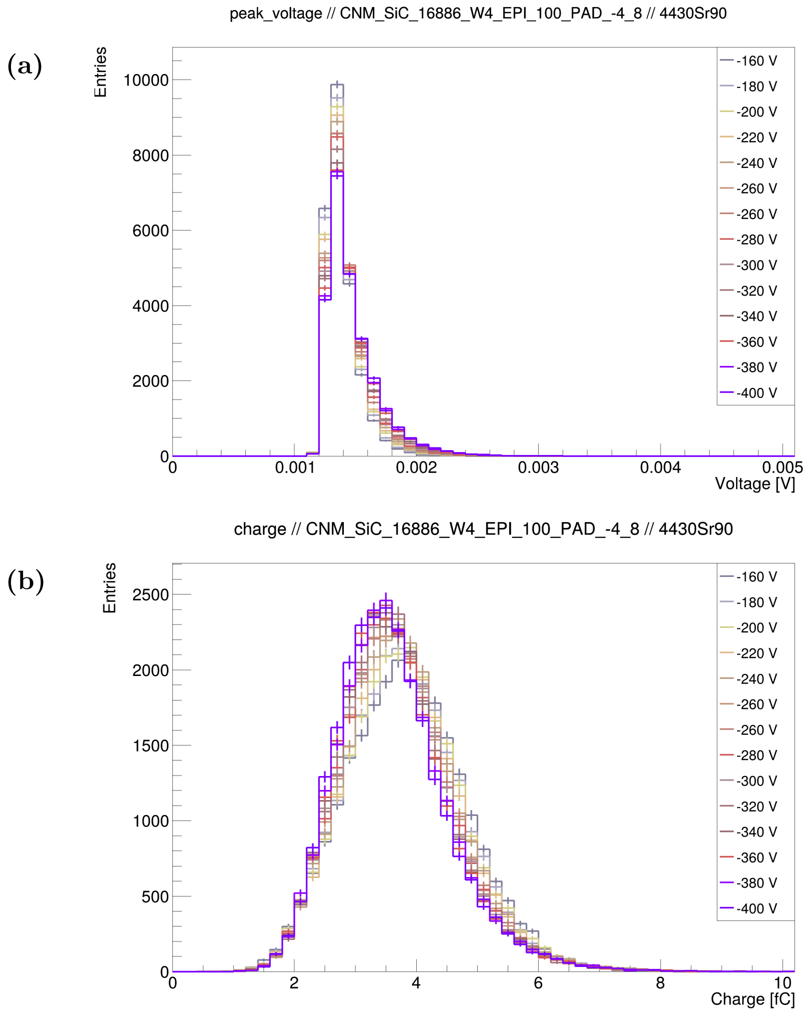

Figure 9: Histograms for (a) peak-voltage and (b) charge for different bias voltages.

4.2 Results for the IHEP sample

Figure 10 shows that for the IHEP sample, the average signals have higher peaks compared to the CNM sample. At higher bias voltages, there is a wide spread of the peak voltages (see Figure 11 (a)). This indicates that particles with a broad range of energies are detected: high-energy particles (strong peak; easy to detect) and, more importantly, also lower-energy particles (corresponding to the peaks just above the trigger level). The wider spread for the IHEP sample than for the CNM sample indicates that the IHEP sample can measure particles with a lower energy than the CNM samples. Nonetheless, there are probably still a lot of β-particles with even lower energy that are not detected by the IHEP sample.

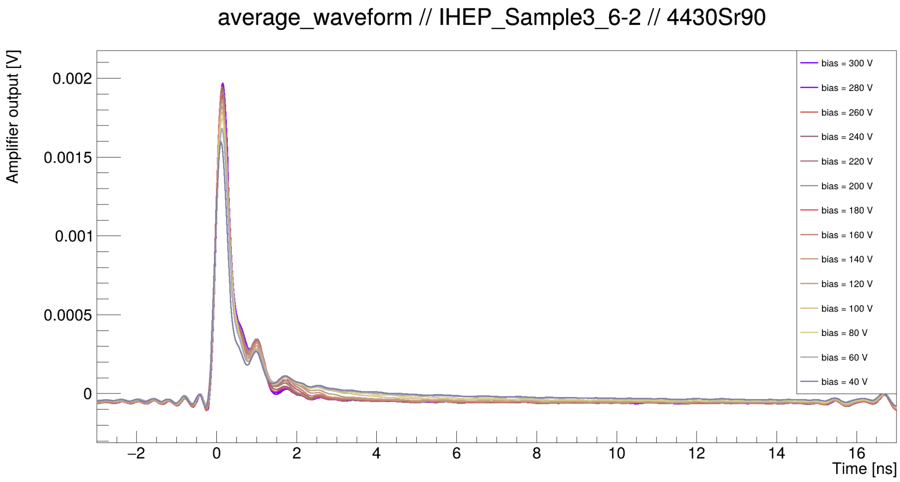

Figure 10: Average of 25’000 recorded waveforms from β-particle detection.

(a)

(b)

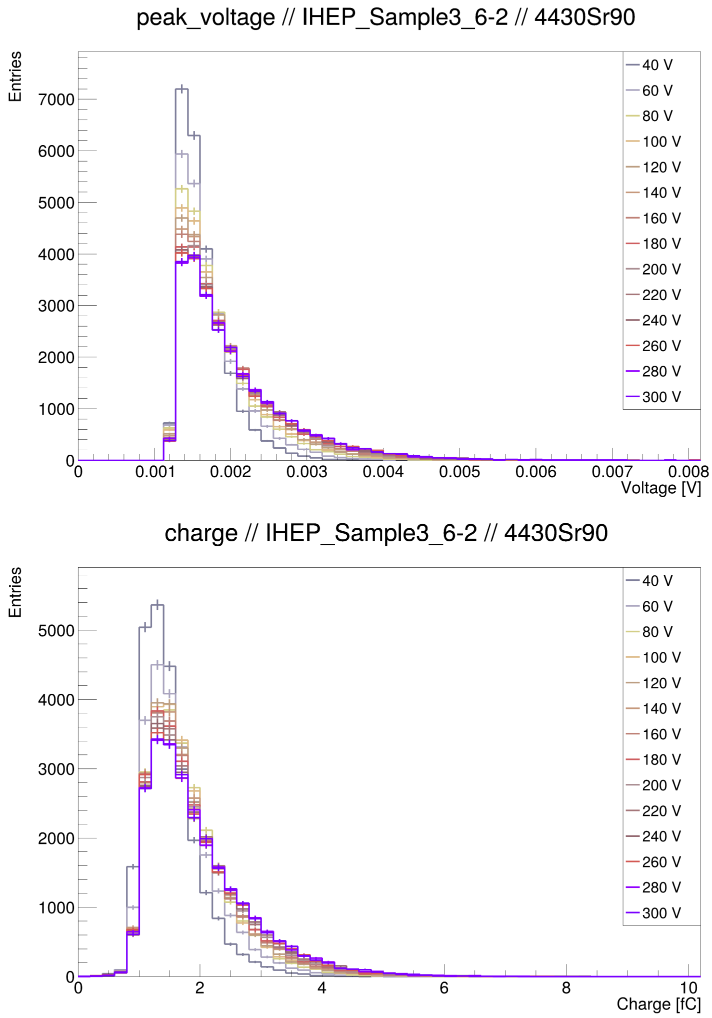

Figure 11: Histograms for (a) peak-voltage and (b) charge for different bias voltages.

5 Conclusion and Outlook

In this project, two SiC pixel detector samples were characterized. First, the noise levels were recorded. Then, the detection capabilities for α- and β-radiation were tested.

The two samples showed comparable performance. They were shown to be capable of reliably detecting α-particles: The signals are clearly above the noise level and the estimated charge is close to the expected value. For β-radiation, some particles can be detected. However, it is very likely that a large share of the β-particles remained undetected because of their lower energy.

The sensitivity could be increased by lowering the oscilloscope trigger level. However, this would also introduce false triggers from noise. A more effective approach for future work could be the implementation of a band-pass filter to suppress frequency components that are characteristic of noise but not of genuine particle-detection events. Additionally, other SiC samples that have not yet been characterized might have improved detection capabilities for β-radiation: a gain layer in the SiC diode could multiply the charge generated in the detector and thus increase the signal strength.

Finally, I would like to thank my supervisors Roman and Susanne for the opportunity to work with them. I had a great time during the CERN Summer Student Programme.

References

[1] ATLAS Collaboration, CERN. (2025) The inner detector. [Online]. Available: https://atlas.cern/Discover/Detector/Inner-Detector

[2] E. Arnqvist, "Characterization of proton irradiated sic sensors," 2023. [Online]. Available: https://repository.cern/records/c15sf-4tx76

[3] M. De Napoli, "Sic detectors: A review on the use of silicon carbide as radiation detection material," *Frontiers in physics*, vol. 10, p. 898833, 2022.

[4] V. Gkougkousis. (2025) Ucsc board specifications. [Online]. Available: https://twiki.cern.ch/twiki/bin/view/Main/UcscSingleChannel

[5] D. Malain and P. Kanchana, "Evaluation of radiation safety for ionization chamber smoke detectors containing am-241," in *Journal of Physics: Conference Series*, vol. 1285, no. 1. IOP Publishing, 2019, p. 012047.

[6] J. Dixon, A. Rajan, S. Bohlemann, D. Coso, A. D. Upadhyaya, A. Rohatgi, S. Chu, A. Majumdar, and S. Yee, "Evaluation of a silicon 90sr betavoltaic power source," *Scientific reports*, vol. 6, no. 1, p. 38182, 2016.